Properties of the optical transitions within the Mn acceptor in $Al_xGa_{1-x}As$

F. Bantien and J. Weber
Max-Planck-Institut für Festkörperforschung, Heisenbergstrasse 1, 7000 Stuttgart 80, Federal Republic of Germany
(Received 9 November 1987)

Manganese-doped $Al_xGa_{1-x}As$ samples are investigated by photoluminescence (PL) measurements. The low-temperature PL spectra exhibit the Mn-related donor-to-acceptor pair transitions $(D^0, A^0)_{Mn}$ for Al concentrations $x \leq 0.42$. The binding energy E_i^{Mn} of the Mn acceptor is determined from the measurements to be $E_i^{Mn} = 0.11 + 0.33x$ eV. $Al_xGa_{1-x}As$ samples with an Al content $x \geq 0.32$ show the intra-atomic $^4T_1 - ^6A_1$ transition of Mn^{2+}. Time-resolved PL measurements give a radiative lifetime of ~ 0.6 ms. Temperature-dependent measurements reveal no shift of the $^4T_1 - ^6A_1$ transition energy with increasing temperature; however, the $^4T_2 - ^6A_1$ transition of Mn^{2+} appears at temperatures higher than 135 K. The crystal-field parameters are estimated from our measurements to be $B = 280\ cm^{-1}$ and $Dq = 300\ cm^{-1}$.

INTRODUCTION

Manganese is an undesired contaminant in all III-V semiconductors. It has a high solubility, and concentrations of up to 10^{20} atoms/cm^3 have been achieved by intentional doping.[1] Manganese can be diffused into the III-V compounds even at low temperatures. The diffusion is fast and seems to be enhanced by intrinsic defects.[1] However, various Mn complexes can be formed during the diffusion process.[2,3]

Atomic manganese is preferentially incorporated in epitaxially grown compounds. Mn substitutes for the group-III metal site and has been found to be an acceptor.[4] The binding energy of the Mn acceptor in the binary compounds ranges from 113 meV in GaAs to ~ 400 meV in GaP.[4-6]

Investigations performed on Mn-doped ternary alloys revealed a linear shift of the Mn binding energy with alloy composition.[7,8] This observation led to the suggestion that the transition-metal level can be used as a common reference energy in all the III-V materials.[9,10] In $Al_xGa_{1-x}As$, however, the shift of the Mn-acceptor level has been found to give a valence-band offset ΔE_v of $\Delta E_v = 0.33x$ eV,[11] which is smaller than the established value of $\Delta E_v \approx 0.45x$ eV.[12]

Photoluminescence (PL) studies on Mn-doped binary III-V compounds revealed various optical transitions. The low-temperature PL spectra of GaAs:Mn and InP:Mn exhibited the donor-to-acceptor pair-transitions $(D^0, A^0)_{Mn}$.[4,13] In Mn-doped GaP, however, the luminescence spectra have been explained by an internal d-shell transition within Mn^{2+} (d^5).[6]

Manganese-related intra-atomic transitions are already known from Mn-doped II-VI compounds.[14,15] The free Mn^{2+} ion has a ^6S ground state, and the first excited state is a ^4G state. A crystal field of cubic symmetry has no influence on the ground state, and this leads to a $^6A_1$ state. The ^4G state is split by the crystal field in a ^4E, $^4A_1$, $^4T_2$, and $^4T_1$ level. The optical spectra have usually been described by electronic transitions between the crystal-field terms of the Mn^{2+} (d^5) ions.[14] The low-energy emission band has been associated with the $^4T_1 - ^6A_1$ transition.[15]

A characteristic property of the intra-atomic $^4T_1 - ^6A_1$ transition is the extremely long radiative lifetime of the excited $^4T_1$ state. The value of ~ 1.2 ms in GaP:Mn is about three orders of magnitude larger than the lifetimes of the $(D^0, A^0)_{Mn}$ transitions in GaAs:Mn and InP:Mn.[6]

The intra-atomic $^4T_1 - ^6A_1$ transition as well as the $(D^0, A^0)_{Mn}$ transition were recently observed in $Al_xGa_{1-x}As$:Mn.[11,16] In the present study, we investigate the simultaneous occurrence of the two different Mn transitions in $Al_xGa_{1-x}As$. We estimate the binding energy of the Mn-acceptor ground state and the position of the excited states with the help of the $(D^0, A^0)_{Mn}$ and the intra-atomic transitions. The properties of the observed Mn transitions are compared with the characteristics of the intra-atomic transition in GaP:Mn. Another Mn-related PL band is observed and we will attribute it to the intra-atomic $^4T_2 - ^6A_1$ transition of Mn^{2+}. Finally, the crystal-field parameters B and Dq are estimated from the experimental values.

EXPERIMENT

The investigated (Al,Ga)As samples are grown by liquid-phase epitaxy from gallium solutions containing ~ 0.1 at. % manganese. Aluminum concentrations of up to 92% are achieved by the epitaxial growth on (100)-oriented semi-insulating GaAs substrates in a conventional graphite slider boat.[17]

Photoluminescence measurements are carried out with the samples either immersed in a liquid-helium bath-cryostat for measurements at ~ 2 K or in a cold-finger cryostat for measurements in the temperature range 8–300 K. The luminescence is excited with different lines of a cw Kr^+ laser, dispersed by a $\frac{3}{4}$-m Spex spectrometer, and recorded with a cooled photomultiplier with an S1 cathode.

Time-resolved PL measurements are performed with

the excitation beam pulsed by an acoustooptic modulator. The luminescence is detected by an S1-cathode photomultiplier and recorded with a digital boxcar analyzer. The lower limit of the time-resolution of the equipment is given by the shortest laser-pulse widths of ~ 20 ns.

RESULTS

The low-temperature PL spectra of Mn-doped $Al_xGa_{1-x}As$ samples with different Al concentrations x are shown in Fig. 1. The excitation density of the focused laser beam is typically ~ 0.5 W/mm^2. The near band-gap energy regime of the GaAs:Mn layer ($x=0$) exhibits the excitonic decay at shallow impurities (~ 820 nm).[18] The donor-to-acceptor pair transitions of the shallow acceptors are found at ~ 830 nm.[19] The pair transitions of the deep Mn acceptor $(D^0, A^0)_{Mn}$ and their phonon replicas are detected at ~ 880 nm wavelength.[4] In contrast to Ref. 20, Mn-related excitonic transitions are not observable.

The optical transitions shift to higher energies with increasing Al content x. According to Ref. 21, we determine x from the energy of the shallow acceptor related excitonic transitions. The energy of the $(D^0, A^0)_{Mn}$-luminescence band depends strongly on the composition x and increases in energy about 270 meV from $x=0$ to $x=0.32$. At $x=0.32$ another Mn-related transition appears at ~ 800 nm wavelength. This broad PL band is due to the internal d-shell transition $^4T_1-^6A_1$ of Mn^{2+}.[11] The $^4T_1-^6A_1$ luminescence band is not observed for Al concentrations $x \leq 0.27$. On the other hand, the $(D^0, A^0)_{Mn}$ transition is not detected under the present excitation conditions in $Al_xGa_{1-x}As$ layers with $x > 0.32$. Only the internal transition is observable in these samples.

We found that a variation in the excitation density results in a pronounced change of the intensity ratio of the two Mn-related PL bands in the sample with $x=0.32$. An increase of the excitation density to ~ 40 W/mm^2 increases the intensity of the $(D^0, A^0)_{Mn}$ luminescence compared to the $^4T_1-^6A_1$ transition. With this excitation, the $(D^0, A^0)_{Mn}$ band is detectable for samples with Al concentrations up to $x=0.42$. On the other hand, a decrease of the excitation density down to ~ 1 μW/mm^2 intensifies the intra-atomic transition compared to the $(D^0, A^0)_{Mn}$ PL band in the samples with $x \geq 0.32$. The $^4T_1-^6A_1$ transition, however, remains undetected in $Al_xGa_{1-x}As$ samples with $x \leq 0.27$ under low-excitation conditions.

The dependence of the Mn-related transition energies $E_{Mn}(D^0, A^0)$ and $E_{Mn}(^4T_1-^6A_1)$ upon the Al concentration x is shown in Fig. 2. The $(D^0, A^0)_{Mn}$ band exhibits a linear shift with x according to

$$E_{Mn}(D^0, A^0) = 1.41 + 0.9x \text{ eV} . \quad (1)$$

The transition energy of the intra-atomic $^4T_1-^6A_1$ transition increases likewise linearly; however, it exhibits a smaller dependence on x:

$$E_{Mn}(^4T_1-^6A_1) = 1.48 + 0.2x \text{ eV} . \quad (2)$$

The significantly long radiative lifetime[6] of the $^4T_1-^6A_1$ transition in GaP:Mn initiated time-resolved PL measurements on the Mn transition in $Al_xGa_{1-x}As$. The radiative decays of different Mn-related PL transitions after pulsed laser excitation are shown in Fig. 3. An exponential decay of the excited Mn state is found for the intra-atomic transitions, whereas the decay curve for pair

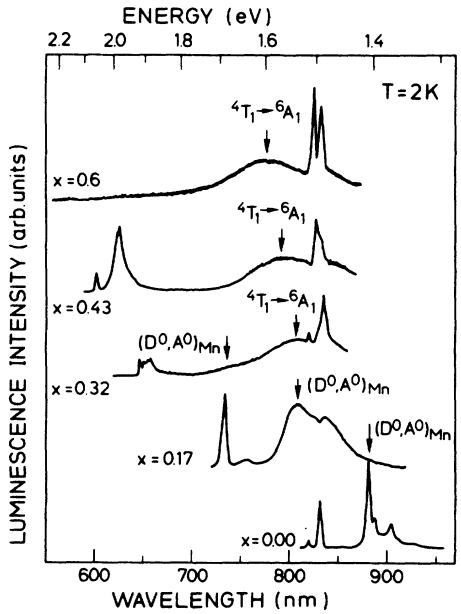

FIG. 1. Low-temperature photoluminescence spectra of $Al_xGa_{1-x}As$:Mn samples with different Al concentrations x. The arrows indicate the Mn-related optical transitions $(D^0, A^0)_{Mn}$ and $^4T_1-^6A_1$.

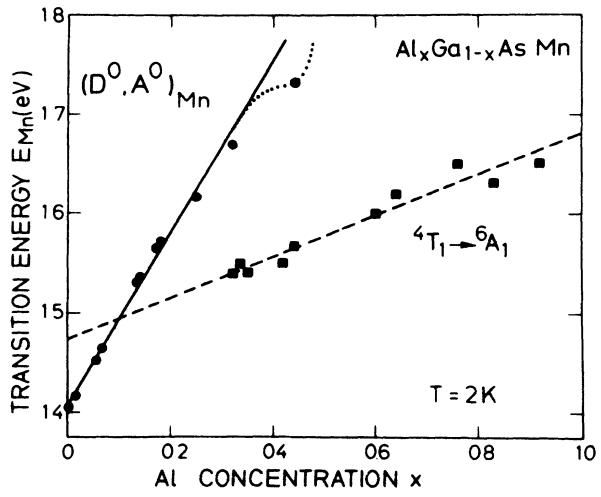

FIG. 2. Dependence of the Mn-related transition energies from the Al concentration x at liquid-helium temperatures. The straight line and full circles present the increase of the $(D^0, A^0)_{Mn}$ transition energy with increasing x. The dotted line takes the nonlinear change of the donor binding energy near $x=0.45$ into account. The dashed line and full squares correspond to the shift of the $^4T_1-^6A_1$ transition energy.

transitions is slightly nonexponential.[22]

The radiative lifetimes τ of the Mn-related transitions are listed in Table I. The lifetimes of the $(D^0, A^0)_{Mn}$ transitions in $Al_xGa_{1-x}As$:Mn with $x \leq 0.32$ are of the order of several microseconds. The values vary from $\tau = 1.5$ μs at $x = 0$ to $\tau = 6.8$ μs at $x = 0.27$. Whereas the intra-atomic $^4T_1 - {}^6A_1$ transitions in $Al_xGa_{1-x}As$:Mn with $x \geq 0.32$ have a much longer lifetime of $\tau \approx 0.6$ ms comparable to the decay times of the intra-atomic transition in GaP:Mn ($\tau \approx 1.2$ ms).

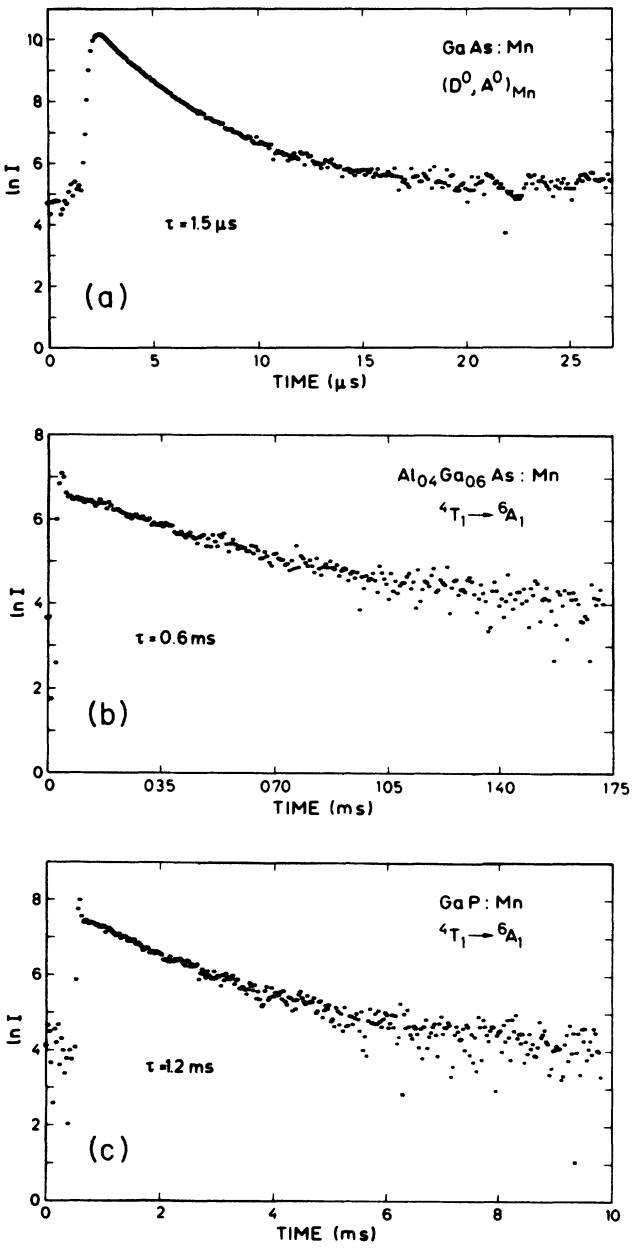

FIG. 3. Decay curves of the Mn-related optical transitions in (a) GaAs:Mn, (b) $Al_xGa_{1-x}As$:Mn, and (c) GaP:Mn at $T = 2$ K. The semilogarithmic plots of the luminescence intensity I vs time show a slightly nonexponential decay for the $(D^0, A^0)_{Mn}$ transition, and exponential decays for the $^4T_1 - {}^6A_1$ transitions.

The PL spectra of $Al_xGa_{1-x}As$:Mn samples which show the intra-atomic Mn transition, are recorded at different sample temperatures. Figure 4 shows the temperature dependence of the luminescence energy of the near-band-gap transition (full squares) and the intra-atomic $^4T_1 - {}^6A_1$ transition (full triangles). The actual Al concentration is $x = 0.42$. The PL energy of the near-band-gap luminescence decreases with increasing temperature according to the Varshni equation:[23]

$$E_g(x,T) = E_g(x,0) - \frac{\alpha T^2}{\beta + T} \ . \tag{3}$$

The band-gap energy $E_g(x,T)$ depends upon the sample temperature T, the parameters α and β, and the band-gap energy $E_g(x,0)$ at $T = 0$ K. The experimental results are in good agreement with the predictions of Eq. (3), when the parameters $\alpha = 5.41 \times 10^{-4}$ eV K^{-1}, $\beta = 290$ K, and $E_g(x,0) = 2.04$ eV are used in analogy to Ref. 21.

The internal d-shell $^4T_1 - {}^6A_1$ transition (full triangles), however, reveals no shift with T. In contrast, the $(D^0, A^0)_{Mn}$ transition energy in GaAs has been found to decrease with increasing T similar to the band-gap energy.[24]

The full circles in Fig. 4 are due to another broad luminescence band which appears at the high-energy tail of the $^4T_1 - {}^6A_1$ transition at higher temperatures. The PL spectra of the corresponding wavelength regime are shown in Fig. 5 for different temperatures. At 135 K, the $^4T_1 - {}^6A_1$ luminescence band at ~ 800 nm (1.55 eV) dominates the spectrum. However, another transition appears at ~ 720 nm (1.72 eV). Even this luminescence band shows a very broad half-width of ~ 100 meV. It increases in intensity compared to the 1.55 eV transition with increasing temperature and dominates the energy regime of the PL spectrum at 185 K. This new transition is found for samples with higher Al concentrations at about the same PL energy. In addition, it shows no energy-shift with increasing temperatures up to 185 K (Fig. 4).

The 1.72-eV transition is found to be Mn related, thus we suggest that the transition occurs from another excited state of Mn^{2+} which is thermally populated at temperatures higher than 135 K. Time-resolved photoluminescence measurements are performed at different temperatures to support our idea of the two intra-atomic Mn transitions. The measured lifetimes are strongly tempera-

TABLE I. Radiative lifetime τ of the Mn-related transition in $Al_xGa_{1-x}As$ for different Al concentrations x.

x	τ (s)	Transition
0	1.5×10^{-6}	$(D^0, A^0)_{Mn}$
0.06	4.2×10^{-6}	
0.17	5.4×10^{-6}	
0.27	6.8×10^{-6}	
0.32	2.4×10^{-6}	
0.32	0.35×10^{-3}	$^4T_1 - {}^6A_1$
0.42	0.60×10^{-3}	
0.64	0.60×10^{-3}	

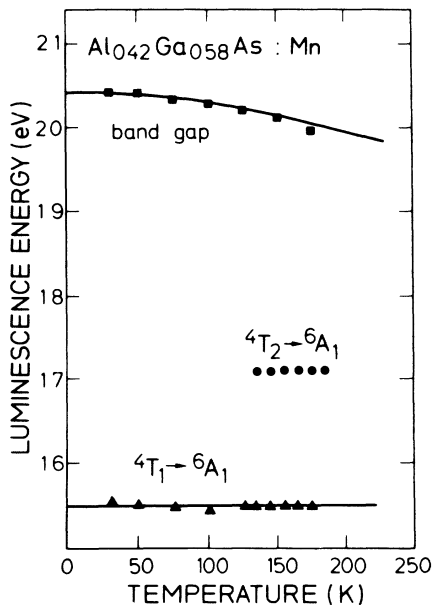

FIG. 4. Temperature dependence of the transition energies for different optical transitions. The near-band-gap luminescence energy (full squares) decreases with increasing T, while the intra-atomic transitions $^4T_1-^6A_1$ (full triangles) and $^4T_2-^6A_1$ (full circles) are temperature independent.

ture dependent. At a given temperature, however, identical lifetimes are found for the 1.55- and 1.72-eV transitions. Our lifetime measurements indicate that both transitions belong to the same thermalizing optical systems.

The temperature dependence of the $^4T_1-^6A_1$ lifetime τ in $Al_{0.4}Ga_{0.6}As$ is given in Fig. 6. At low temperatures,

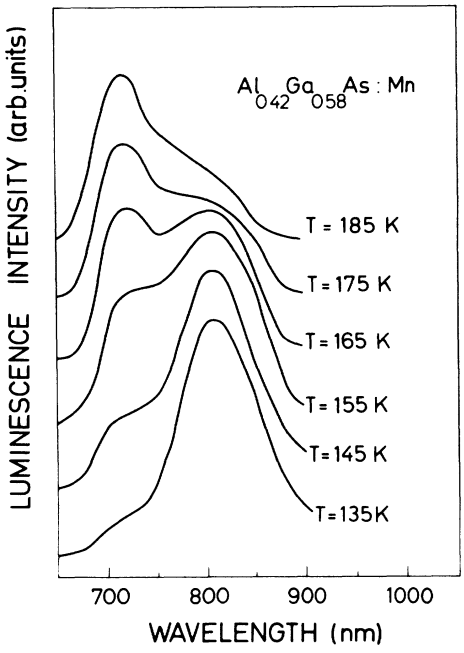

FIG. 5. Photoluminescence spectra of the intra-atomic optical transitions in Mn-doped $Al_xGa_{1-x}As$ recorded at different temperatures T.

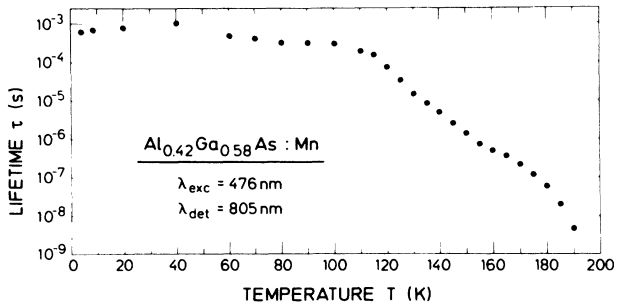

FIG. 6. Temperature dependence of the measured lifetime in $Al_xGa_{1-x}As$:Mn for the $^4T_1-^6A_1$ transition.

the lifetime is 0.6 ms. This value corresponds to the radiative lifetime of the spin-forbidden optical transition. The measured lifetime remains constant when increasing the temperature to about 100 K and decreases very rapidly in the temperature regime from 100 K to 200 K. The measured value at 190 K is more than 5 orders of magnitude smaller than the low-temperature value.

The decrease in lifetime occurs in the same temperature regime, where the second internal transition ($^4T_2-^6A_1$) appears in the PL spectra. The temperature-dependence of the measured lifetimes can be explained by assuming an optical transition scheme of two thermalizing initial states ($^4T_1$ and $^4T_2$) and different transition probabilities to the $^6A_1$ ground state.[25] We obtain a reasonable fit of the experimental decay times by using a radiative lifetime of 0.6 ms for the $^4T_1-^6A_1$ transition and a value of $\sim 10^{-11}$ s for the $^4T_2-^6A_1$ transition. However, this value seems to be too small to account for a spin-forbidden crystal-field transition. We therefore assume that a very efficient transfer process (e.g., to the conduction band) is thermally activated, which reduces the decay times by orders of magnitude.

DISCUSSION

The nature of the Mn acceptor in GaAs has been in debate for a long time. It was unclear whether the acceptor should be described by a localized hole in the d shell, resulting in a d^4 configuration,[26] or due to a loosely bound hole which gives a (d^5+h) configuration.[27]

Recent EPR studies by Schneider *et al.*[28] showed, that the negatively charged core of the Mn acceptor (Mn^{2+}) consists of five d electrons $[A^-(d^5)]$. The ground state of the core is $S=\frac{5}{2}$ ($^6A_1$) and the different excited states ($^4T_1, ^4T_2, ^4E, ^4A_1$) originate from the crystal-field-split atomic state ^4G. In the neutral state of the acceptor a more delocalized hole with $j=\frac{3}{2}$ is bound to the negatively charged core.

In the (D^0, A^0) pair transitions, the donor-electron recombines with the weakly bound hole, leaving the d shell unaffected. However, the internal transition within the d shell is observed in the crystal-field-split manifold of the d^5 shell. The bound hole seems to be unaffected by this internal transition.

Our low-temperature photoluminescence studies on Mn-doped $Al_xGa_{1-x}As$ suggest that the first excited

Mn^{2+} state happens to be degenerate with the conduction band in GaAs. The excitation of one of the $(3d)^5$ electrons from the $^6A_1$ ground state into the excited $^4T_1$ state results therefore in a charge-transfer process, where the excited electron is emitted into the conduction band. The PL measurements exhibit no internal d-shell transitions, however, the $(D^0, A^0)_{Mn}$ pair transitions occur.

The $^4T_1$ level shifts towards the conduction-band minimum with increasing Al concentration up to $x=0.27$. Thus the excited Mn^{2+} level is still degenerate with the conduction band, as is shown schematically in Fig. 7. The PL spectra reveal only the $(D^0, A^0)_{Mn}$ transition. From these measurements, the binding energy $E_i^{Mn}(x)$ of the Mn-acceptor ground state in $Al_xGa_{1-x}As$ can be determined.

The binding energy of the Mn acceptor at liquid-helium temperatures is, according to Ref. 29, given by

$$E_i^{Mn}(x)=E_g(x)-E_{Mn}(D^0, A^0)-E_i^D(x)+\Delta E \ . \quad (4)$$

The band-gap energy $E_g(x)$ and the binding energy of the neutral donor $E_i^D(x)$ are well known in the desired Al-concentration regime.[21] The pairing interaction term ΔE represents the Coulomb interaction between the impurity levels[29] and is typically of the order of 10 meV for our samples. We fit the binding energy of the Mn acceptor in $Al_xGa_{1-x}As$ from our measurements and find

$$E_i^{Mn}=0.11+0.33x \text{ eV} \ . \quad (5)$$

The radiative lifetime of the Mn-related pair transitions depends on the binding energy of the Mn acceptor and the strength of the pairing interaction.[22] The measured lifetimes of pair transitions in GaAs are ~ 1 μs for the shallow acceptors. Because of the increased binding energy, the $(D^0, A^0)_{Mn}$ transitions have a longer lifetime of 1.5 μs. The increase of the Mn binding energy in $Al_xGa_{1-x}As$ with increasing x leads again to a longer lifetime of the $(D^0, A^0)_{Mn}$ transitions in the μs regime, as is shown in Table I. The relatively short lifetime of the $(D^0, A^0)_{Mn}$ transition in the $Al_xGa_{1-x}As$ layer with $x=0.32$, however, results from a slightly higher Mn concentration within this sample. The increase of the doping concentration strengthens the pairing interaction and intensifies therefore the pair-recombination probability.

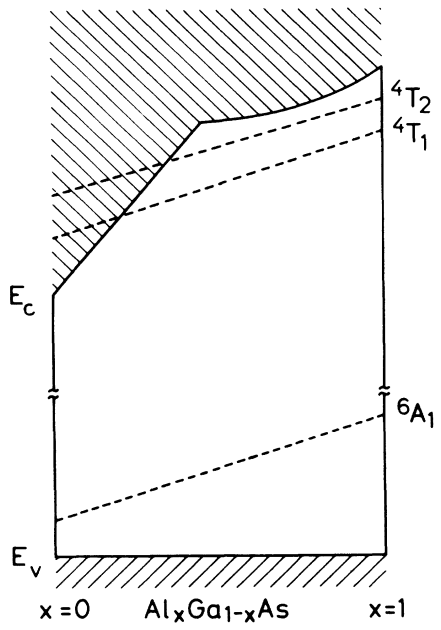

FIG. 7. Model of the $Al_xGa_{1-x}As$:Mn energy levels. E_v and E_c label the valence- and conduction-band edges, respectively. The dashed lines represent the Mn-related energy levels $^6A_1$, $^4T_1$, and $^4T_2$.

For $x>0.3$, the pair transition furthermore shifts to higher energies with increasing Al concentration (Fig. 2); however, the transition energy of the $(D^0, A^0)_{Mn}$ PL band does not exactly follow Eq. (1). the increase of the donor binding energy[21] from ~ 5 meV at $x=0.3$ to ~ 55 meV at $x=0.42$ reduces the high-energy shift of $E_{Mn}(D^0, A^0)$. The expected transition energy is shown by the dashed line in Fig. 2.

The $^4T_1$ state of Mn^{2+} interchanges with the conduction-band minimum somewhere between $x=0.27$ and $x=0.32$ (Fig. 7). While the $Al_xGa_{1-x}As$ samples with $x \leq 0.27$ exhibit only the $(D^0, A^0)_{Mn}$ transition, the excitation of samples with $x \geq 0.32$ results in two different PL bands. Besides the pair transition, the intra-atomic $^4T_1-^6A_1$ transition of Mn^{2+} is activated. A further increase of the Al concentration x increases the $Al_xGa_{1-x}As$ band-gap energy, and the $^4T_1$ state shifts more and more into the gap (Fig. 7). Thus the difference between the intra-atomic and the pair-transition energy increases with increasing x.

Our low-temperature lifetime measurements give a radiative lifetime of ~ 0.6 ms for the $^4T_1-^6A_1$ transition in $Al_xGa_{1-x}As$:Mn (Table I). This value is similar to the value for GaP:Mn and confirms the assignment of the PL band to the intra-atomic transition.

The transition energy of internal d-shell transitions are nearly independent of the sample temperature. The PL line width of the luminescence band increases with increasing temperature, due to the Boltzmann population of the excited state. This corresponds to our observations on the $^4T_1-^6A_1$ transition in $Al_xGa_{1-x}As$:Mn (Figs. 4 and 5) and proves our interpretation of an intra-atomic transition, whereas the $(D^0, A^0)_{Mn}$ transition behaves differently GaAs:Mn.[24]

Another Mn-related transition is observed at 1.72 eV for higher temperatures (Fig. 5). The lifetimes of the 1.72-eV PL band and the $^4T_1-^6A_1$ transition are found to be identical at certain temperatures. This shows that both of the transitions belong to the same luminescent center. We therefore suggest that even this PL band corresponds to an intra-atomic transition of Mn^{2+}.

The 1.72-eV transition appears only at temperatures $T \geq 135$ K. We assume that it occurs from another excited state of Mn^{2+} which is thermally populated from the $^4T_1$ state. From the Tanabe-Sugano diagram,[30] we find the second excited state to be a $^4T_2$ level. The 1.72-eV PL band should therefore correspond to the $^4T_2-^6A_1$ transition of Mn^{2+}.

At temperatures $T \geq 165$ K, the luminescence intensity of the $^4T_2-^6A_1$ transition exceeds the $^4T_1-^6A_1$ intensity.

We interpret this observation with the different transition probabilities of the two transitions. While both of the Mn^{2+} transitions are spin forbidden, only the $^4T_2-{}^6A_1$ transition is crystal-field allowed in T_d symmetry. The different recombination probabilities therefore give rise to an enhanced luminescence intensity of the $^4T_2-{}^6A_1$ transition at higher temperatures.

We want to estimate the values of the crystal-field parameters B and Dq which are used in the Tanabe-Sugano diagram.[30] In a simple first-order estimate, we determine the crystal-field parameters from the maxima of the two broad PL bands. Using the samples with $x \approx 0.4$, we find $B = 280 \pm 30$ cm^{-1} and $Dq = 300 \pm 10$ cm^{-1}. The values for B and Dq are nearly a factor of two smaller than those found for Mn in the II-VI compound semiconductors[14,15] and for Mn in GaP.[6] Presently we have no explanation for this reduction.

A much better estimate for the crystal-field parameters should be obtained by using the zero-phonon energies. Unfortunately, zero-phonon transitions have not been observed up to now. However, the zero-phonon energy of the $^4T_1-{}^6A_1$ transition can roughly be deduced at $x \approx 0.3$. Our PL measurements suggest that the actual Al concentration x_i of the interchange between the $^4T_1$ state and the conduction-band minimum is $x_i = 0.30 \pm 0.02$. The $(D^0, A^0)_{Mn}$ transition energy at $x = x_i$ determines the zero-phonon energy $E_{ZP}^{(^4T_1-{}^6A_1)}$ of the intra-atomic transition $^4T_1-{}^6A_1$, because the $^4T_1$ state and the conduction-band minimum, or the D^0 level are degenerate. We therefore calculate the zero-phonon energy from Eq. (1). At the Al concentration x_i, we obtain

$$E_{ZP}^{(^4T_1-{}^6A_1)}(x_i) = 1.67 \pm 0.03 \text{ eV} . \quad (6)$$

The energy of the maximum of the $^4T_1-{}^6A_1$ PL band at $x = x_i$, however, as determined from Eq. (2), is 1.54 eV, which gives a Stoke's shift of ~ 130 meV in $Al_{0.3}Ga_{0.7}As$:Mn. This is similar to the value of 110 meV found for GaP:Mn.[6] We expect a similar Stoke's shift for $Al_{0.4}Ga_{0.6}As$:Mn and assume the same value for the $^4T_2-{}^6A_1$ transition. From these estimates, we get similar crystal-field parameters as calculated above.

CONCLUSIONS

Manganese-related optical transitions in $Al_xGa_{1-x}As$:Mn are investigated by PL measurements. The $(D^0, A^0)_{Mn}$ transitions are observed for Al concentrations $x \leq 0.42$. From these measurements, the binding energy of the Mn acceptor is found to be $E_i^{Mn} = 0.11 + 0.33x$ eV.

The excited $^4T_1$ state of Mn^{2+} is degenerate with the conduction band in $Al_xGa_{1-x}As$ with low Al concentrations. It interchanges with the conduction-band minimum at $x \approx 0.3$ and gives rise to the intra-atomic $^4T_1-{}^6A_1$ transition found for samples with higher Al concentrations. Optical transitions from another excited state Mn^{2+} have been observed. They are attributed to the $^4T_2-{}^6A_1$ transition, which is activated at higher temperatures.

The radiative lifetimes of the Mn-related transitions are found to be 1–7 μs for the $(D^0, A^0)_{Mn}$ and 600 μs for the $^4T_1-{}^6A_1$ transition. At temperatures $T > 100$ K, the measured lifetime of the intra-atomic transition decreases rapidly, due to thermally activated transfer processes. The crystal-field parameters are calculated from our measurements. We find $B = 280$ cm^{-1} and $Dq = 300$ cm^{-1}.

ACKNOWLEDGMENTS

We thank E. Bauser and H. J. Queisser for their interest and support of this work, and W. Heinz for his technical assistance.

[1] Y. Sasaki, T. Sato, K. Matsushita, T. Harin, and Y. Shibata, J. Appl. Phys. **57**, 1109 (1985).
[2] R. S. Title, J. Appl. Phys. **40**, 4902 (1969).
[3] K. H. Segsa and S. Spenke, Phys. Status Solidi A **27**, 129 (1975).
[4] W. Schairer and M. Schmidt, Phys. Rev. B **10**, 2501 (1974).
[5] L. Eaves, A. W. Smith, M. S. Skolnick, and B. Cockayne, J. Appl. Phys. **53**, 4955 (1982).
[6] A. T. Vink and G. G. P. van Gorkom, J. Lumin. **5**, 379 (1972).
[7] L. Samuelson, M.-E. Pistol, and S. Nilsson, Phys. Rev. B **33**, 8776 (1986).
[8] S. Nilsson and L. Samuelson, *Materials Science Forum*, edited by H. J. von Bardeleben (Trans Tech Publications Ltd., Zurich, Switzerland, 1986), Vols. 10–12, p. 615.
[9] J. M. Langer and H. Heinrich, Phys. Rev. Lett. **55**, 1414 (1985).
[10] J. Tersoff, Phys. Rev. Lett. **56**, 675 (1986).
[11] F. Bantien and J. Weber, Solid State Commun. **61**, 423 (1987).
[12] M. Cardona and N. E. Christensen, Phys. Rev. B **35**, 6182 (1987).
[13] B. Plot-Chan, B. Deveaud, A. Rupert, and B. Lambert, J. Phys. C **18**, 5651 (1985).
[14] H. E. Gumlich, R. L. Pfrogner, J. C. Shaffer, and F. E. Williams, J. Chem. Phys. **44**, 3929 (1966).
[15] D. W. Langer and H. J. Richter, Phys. Rev. **146**, 554 (1966).
[16] B. Plot, B. Deveaud, B. Lambert, A. Chomette, and A. Regreny, J. Phys. C **19**, 4279 (1986).
[17] P. Zwicknagl, W. Rehm, and E. Bauser, J. Electron. Mater. **13**, 545 (1984).
[18] E. H. Bogardus and H. B. Bebb, Phys. Rev. **176**, 993 (1968).
[19] D. J. Ashen, P. J. Dean, D. T. J. Hurle, J. B. Mullin, and A. M. White, J. Phys. Chem. Solids **36**, 1041 (1975).
[20] S. Bilac, Z. P. Argüeelo, C. A. Argüello, and R. C. C. Leite, Solid State Commun. **25**, 755 (1978).
[21] S. Adachi, J. Appl. Phys. **58**, R1 (1985).
[22] D. G. Thomas, J. J. Hopfield and W. M. Augustyniak, Phys. Rev. A **140**, 202 (1965).
[23] Y. P. Varshni, Physica (Utrecht) **34**, 149 (1967).
[24] P. W. Yu and Y. S. Park, J. Appl. Phys. **50**, 1097 (1979).
[25] J. D. Cuthbert and D. G. Thomas, Phys. Rev. **154**, 763 (1967).
[26] D. G. Andrianov, Yu. A. Grigorev, S. O. Klimonskii, A. S.

Savelev, and S. M. Yakubenya, Fiz. Tekh. Poluprovodn. **18**, 262 (1984) [Sov. Phys.—Semicond. **18**, 162 (1984)].
[27]U. Kaufmann and J. Schneider, Adv. Electron. Electron Phys. **58**, 81 (1982).
[28]J. Schneider, U. Kaufmann, W. Wilkening, M. Baeumler, and F. Köhl, Phys. Rev. Lett. **59**, 240 (1987).
[29]J. I. Pankove, *Optical Processes in Semiconductors* (Dover, New York, 1975).
[30]Y. Tanabe and S. Sugano, J. Phys. Soc. Jpn. **9**, 766 (1954).